Vol 16 No 11, November 2007
1009-1963/2007/16(11)/3290-07

Chinese Physics

© 2007 Chin. Phys. Soc.
and IOP Publishing Ltd

Hyperon coupling dependence of hadron matter properties in relativistic mean field model*

Mi Ai-Jun(米爱军)[a)†], Zuo Wei(左 维)[a)b)], and Li Ang(李 昂)[c)]

[a)] *School of Nuclear Science and Technology, Lanzhou University, Lanzhou* 730000, *China*
[b)] *Institute of Modern Physics, Chinese Academy of Sciences, Lanzhou* 730000, *China*
[c)] *School of Physical Science and Technology, Lanzhou University, Lanzhou* 730000, *China*

(Received 19 December 2006; revised manuscript received 22 February 2007)

The properties of hadronic matter at β equilibrium in a wide range of densities are described by appropriate equations of state in the framework of the relativistic mean field model. Strange meson fields, namely the scalar meson field $\sigma^*(975)$ and the vector meson field $\phi(1020)$, are included in the present work. We discuss and compare the results of the equation of state, nucleon effective mass, and strangeness fraction obtained by adopting the TM1, TMA, and GL parameter sets for nuclear sector and three different choices for the hyperon couplings. We find that the parameter set TM1 favours the onset of hyperons most, while at high densities the GL parameter set leads to the most hyperon-rich matter. For a certain parameter set (e.g. TM1), the most hyperon-rich matter is obtained for the hyperon potential model. The influence of the hyperon couplings on the effective mass of nucleon, is much weaker than that on the nucleon parameter set. The nonstrange mesons dominate essentially the global properties of dense hyperon matter. The hyperon potential model predicts the lowest value of the neutron star maximum mass of about $1.45\,M_{\rm sun}$ to be 0.4–0.5 $M_{\rm sun}$ lower than the prediction by using the other choices for hyperon couplings.

Keywords: hyperon coupling, strange meson field, equations of state
PACC: 1375E, 2165, 9160F, 9760J

The properties and composition of dense hadronic matter at supranuclear densities are crucial to the static and dynamical behaviour of stellar matter. It is universally received that at extremely high densities, strangeness may occur in the form of hadrons (such as hyperons and/or a K^- meson condensation) or in the form of strange quarks. Since the strong interaction plays an important role in determining the structure of hadronic matter at high densities, the theoretical models used to describe it should reflect the main feature of the theorem of strong interaction predicted by quantum chromodynamics (QCD). Along this line, the relativistic mean field (RMF) model was used first by Glendenning for describing the matter with hyperons[1−3] and improved later. In addition to the usual σ, ω and ρ mesons[4−10] two strange mesons σ^* and ϕ have been introduced[11−14] to reproduce the experimental hyperon–hyperon interactions.

In the framework of the RMF model, many studies have been done.[11−24] Authors in Ref.[15] demonstrated the importance of the σ^* and ϕ mesons by investigating the influence of strange mesons on the equation of state (EOS) and properties of neutron star matter. They also found that the inclusion of the hyperon–hyperon interaction makes the onset of the kaon condensation less favourable. The studies in Refs.[21, 23] show that the effects of hyperon couplings are significant only at densities much larger than the nuclear matter saturation density. In Ref.[22], it is shown that the contribution from hyperons is quite sensitive to the hyperon couplings. Since all these studies indicate that the hyperon–hyperon interactions play an important role in predicting the properties of hadronic neutron star matter, a systemic investigation of the effect of the hyperon couplings is necessary.

The onset of hyperons depends on not only the conditions of chemical equilibrium and charge neutrality discussed below but also the meson–hyperon coupling constants, which are still very controversial

*Project supported by the National Natural Science Foundation of China (Grant Nos 10575119 and 10235030), the Knowledge Innovation Program of Chinese Academy of Sciences (Grant No KJCX2-SW-N02), the State Key Development Program for Basic Research of China (Grant No G2000077400), the Key Preresearch Program of the Ministry of Science and Technology of China (Grant No 2002CCB00200), and the Asia–Europe Link project of the European Commission (Grant No CN/ASIA-LINK/008(94791)).
†E-mail: miaj05@lzu.cn

due to the rare hyperon experimental data. There are several ways to introduce the meson–hyperon coupling constants, i.e. to obtain the following quantities: $x_\sigma = g_{Y\sigma}/g_{N\sigma}$, $x_\omega = g_{Y\omega}/g_{N\omega}$ and $x_\rho = g_{Y\rho}/g_{N\rho}$ (where $g_{\rm BM}$ is the coupling constant of the baryon B with the meson M, and $g_{\rm NM}$ refers to the nucleon–meson couplings.). Choosing the scalar coupling constants fixed to hypernuclear data, Schaffner *et al* have performed a full investigation of the phase transition to hyperonic matter and the EOS of hyperon-rich matter in neutron stars.[13−16] The value of x_σ, determined in this way, is about 0.62, and the vector coupling constants are chosen according to the quark model. The so-called quark counting choice ($x_\sigma = x_\omega = x_\rho = \sqrt{2/3}$) has been widely used in Refs.[17–20] to study the properties of strange hadronic matter containing hyperons (Λ, Σ, Ξ). In Ref.[21], the authors have explored the matter properties beyond this scale, that is $x_\sigma = x_\omega = x_\rho = 1$, the universal coupling. In addition, the hyperon coupling constants constrained by quark model are also commonly used.[22] The big difference between the definitions of the meson–hyperon couplings in the literature has motivated us to investigate the potentially crucial influences of it. We address here this crucial problem by examining specifically the hyperon-coupling dependence of the matter properties for three different sets of the hyperon couplings, namely the quark counting choice, the universal coupling choice and the hyperon potential model choice. In the first two cases we extend the former rule and let the value of σ^* (ϕ) meson couplings equal those of the σ (ω). For the hyperon potential model choice, the coupling constants of hyperons with the scalar σ and σ^* mesons are constrained by the hyperon potentials compatible with hypernuclear data:[16,24] $U_\Lambda^{(\rm N)}(\rho_0) = -30\,{\rm MeV}$, $U_\Sigma^{(\rm N)}(\rho_0) = 30\,{\rm MeV}$, $U_\Xi^{(\rm N)}(\rho_0) = -18\,{\rm MeV}$, and $U_\Xi^{(\Xi)}(\rho_0) \simeq U_\Lambda^{(\Xi)}(\rho_0) \simeq 2U_\Xi^{(\Lambda)}(\rho_0) \simeq 2U_\Lambda^{(\Lambda)}(\rho_0) \simeq -40\,{\rm MeV}$. Here $U_i^{(j)}$ denotes the potential well depth of a baryon species i in the matter made up of a baryon species j. The coupling constants of hyperons with the vector mesons ω, ρ, ϕ are fixed by using SU(6) symmetry.[22]

We first review briefly the extended RMF model including hyperons adopted in our calculation, then apply it to the study of the properties of strange hadronic matter. Finally a summary of the present work is given.

The Lagrangian of the theory is

$$\begin{aligned}\mathcal{L}_B = \sum_B \bar\psi_B(&{\rm i}\gamma^\mu\partial_\mu - g_{\omega B}\gamma^\mu V_\mu - g_{\phi B}\gamma^\mu\phi_\mu\\ &-g_{\rho B}\gamma^\mu\tau^a\rho_\mu^a - M_B + g_{sB}\sigma + g_{\sigma^* B}\sigma^*)\psi_B\\ &-\frac{1}{4}G_{\mu\nu}G^{\nu\mu} + \frac{1}{2}m_\omega^2 V_\mu V^\mu + \frac{1}{4}c_3\left(V_\mu V^\mu\right)^2\\ &+\frac{1}{2}\partial_\mu\sigma\partial^\mu\sigma - \frac{1}{2}m_\sigma^2\sigma^2 - \frac{1}{3}g_2\sigma^3 - \frac{1}{4}g_3\sigma^4\\ &-\frac{1}{4}R_{\mu\nu}^a R^{a\mu\nu} + \frac{1}{2}m_\rho^2\rho_\mu^a\rho^{a\mu}\\ &-\frac{1}{4}S_{\mu\nu}S^{\mu\nu} + \frac{1}{2}m_\phi^2\phi_\mu\phi^\mu\\ &+\frac{1}{2}\left(\partial_\nu\sigma^*\partial^\nu\sigma^* - m_{\sigma^*}^2\sigma^{*^2}\right),\end{aligned} \tag{1}$$

where $G_{\mu\nu} = \partial_\mu V_\nu - \partial_\nu V_\mu$, $S_{\mu\nu} = \partial_\mu\phi_\nu - \partial_\nu\phi_\mu$ and $R_{\mu\nu}^a = \partial_\mu\rho_\nu^a - \partial_\nu\rho_\mu^a + g_\rho\varepsilon_{abc}\rho_\mu^b\rho_\nu^c$ are the ω field, ϕ field and ρ field strength tensors, respectively. We take three parameter sets (namely, TM1,[25,26] TMA,[27] GL[2]) as the nuclear sector in the above Lagrangian, which are expected to provide reasonable descriptions of the properties of dense matter in a wide range of densities relevant to astrophysical interests.

For an infinite matter, one may introduce the mean field approximation. Under the mean field approximation, the meson fields are replaced by their mean values and the equations of motion can be simplified into

$$m_\sigma^2\sigma + g_2\sigma^2 + g_3\sigma^3 = \sum_B g_{\sigma B}\frac{2J_B+1}{2}n_B^{\rm s}, \tag{2}$$

$$m_\omega^2\omega + c_3\omega^3 = \sum_B g_{\omega B}\left(2J_B+1\right)k_B^3/(6\pi^2), \tag{3}$$

$$m_\rho^2\rho = \sum_B g_{\rho B}I_{3B}\left(2J_B+1\right)k_B^3/(6\pi^2), \tag{4}$$

$$m_{\sigma^*}^2\sigma^* = \sum_B g_{\sigma^* B}\frac{2J_B+1}{2}n_B^{\rm s}, \tag{5}$$

$$m_\phi^2\phi = \sum_B g_{\phi B}\left(2J_B+1\right)k_B^3/(6\pi^2), \tag{6}$$

where k_B is the Fermi momentum of the baryon species B, and $J_{\rm B}$ and $I_{3\rm B}$ denote the spin and the isospin z-projections of the baryon B, respectively. The baryon scalar density $n_B^{\rm s}$ is defined as

$$n_B^{\rm s} = \frac{1}{\pi^2}\int_0^{k_B}{\rm d}k\,k^2\frac{m_B^*}{\sqrt{m_B^{*2}+k_B^2}}, \tag{7}$$

where

$$m_B^* = m_B - g_{\sigma B}\sigma - g_{\sigma^* B}\sigma^* \tag{8}$$

is the effective mass of the baryon species B. The ω, ρ and ϕ fields can be obtained respectively by expressions (3), (4) and (6). The scalar fields σ and σ^* can be determined by solving iteratively the coupled expressions (2), (5), (7) and (8).

For a neutron star matter with uniform distributions, the composition is determined by meeting the

requirements for charge neutrality and β-equilibrium conditions. The charge neutrality requires

$$n_{\rm p} + n_{\Sigma^+} = n_{\rm e} + n_{\mu} + n_{\Sigma^-} + n_{\Xi^-}, \tag{9}$$

and the β-equilibrium conditions in the weak processes (B_1 and B_2 denote baryons) are

$$B_1 \to B_2 + L, \quad \text{and} \quad B_2 + L \to B_1,$$

which lead to the following relations among the involved chemical potentials:

$$\mu_{\rm p} = \mu_{\Sigma^+} = \mu_{\rm n} - \mu_{\rm e},\ \mu_{\Lambda} = \mu_{\Sigma^0} = \mu_{\Xi^0} = \mu_{\rm n},$$

$$\mu_{\Sigma^-} = \mu_{\Xi^-} = \mu_{\rm n} + \mu_{\rm e},\ \mu_{\mu} = \mu_{\rm e}. \tag{10}$$

Specially, one can define the parameter fs to specify the strangeness content in the system

$$fs = \frac{n_{\rm s}}{n_{\rm b}} = \frac{n_{\Lambda} + n_{\Sigma} + 2n_{\Xi}}{n_{\rm b}}, \tag{11}$$

which may be regarded as another important degree of freedom, similar to the nuclear asymmetry $\beta = N/Z$. The total energy density ε and the pressure P of the uniform matter are given respectively by

$$\varepsilon = \sum_B \frac{2J_B+1}{2\pi^2}\int_0^{k_B}\sqrt{k^2+m_B^{*2}}\ k^2{\rm d}k + \frac{1}{2}m_\sigma^2\sigma^2 + \frac{1}{3}g_2\sigma^3 + \frac{1}{4}g_3\sigma^4 + \frac{1}{2}m_\omega^2\omega^2 + \frac{3}{4}c_3\omega^4 + \frac{1}{2}m_\rho^2\rho^2 + \frac{1}{2}m_{\sigma^*}^2\sigma^{*2} + \frac{1}{2}m_\phi^2\phi^2 + \sum_l \frac{1}{\pi^2}\int_0^{k_l}\sqrt{k^2+m_l^2}\ k^2{\rm d}k, \tag{12}$$

$$P = \frac{1}{3}\sum_B \frac{2J_B+1}{2\pi^2}\int_0^{k_B}\frac{k^4{\rm d}k}{\sqrt{k^2+m_B^{*2}}} - \frac{1}{2}m_\sigma^2\sigma^2 - \frac{1}{3}g_2\sigma^3 - \frac{1}{4}g_3\sigma^4 + \frac{1}{2}m_\omega^2\omega^2 + \frac{1}{4}c_3\omega^4 + \frac{1}{2}m_\rho^2\rho^2 - \frac{1}{2}m_{\sigma^*}^2\sigma^{*2} + \frac{1}{2}m_\phi^2\phi^2 + \frac{1}{3}\sum_l \frac{1}{\pi^2}\int_0^{k_l}\frac{k^4{\rm d}k}{\sqrt{k^2+m_l^2}}\ . \tag{13}$$

We begin with the discussion of the influence of the nucleon–meson couplings on the composition of neutron star matter. Figure 1 shows the relative populations of nucleons, hyperons, electrons, and muons in β-equilibrium neutron star matter obtained by adopting the three different parameter sets TM1 (top panel), TMA (middle panel), and GL (lower panel) for the nucleon interaction and the quark counting choice for the hyperon interaction. One can see clearly that both the thresholds and populations of hyperons predicted by the TM1, TMA and GL parameter sets are quite different from each other. The negatively charged Σ^- with a mass of 1193 MeV and the neutral Λ with a mass of 1116 MeV appear first, at densities of 0.25–0.35 fm^{-3} for all the three kinds of parameter sets. Their onsets appear to be slightly earlier in the case of using the TM1 parameter set. The negatively charged Σ^- is the main reason for $\mu_{\rm e}$ to fall with density (shown clearly in Fig.3 below). For the TM1 and TMA parameter sets, the Σ^- population grows faster than the Λ population. The Σ^- population is saturated at $\rho \sim 0.55$ fm^{-3} for the TM1 case and at $\rho \sim 0.64$ fm^{-3} for the TMA case. Whereas, for the GL parameter set, the Λ hyperon becomes the most abundant hyperon in the density region of $\rho > 0.64$ although the Σ^- hyperon is more abundant than the Λ at lower densities. Furthermore, another negatively charged Ξ^- with a mass of 1313 MeV appears at almost the same density value ($\rho \sim 0.62$ fm^{-3}) for the TMA and GL parameter sets,

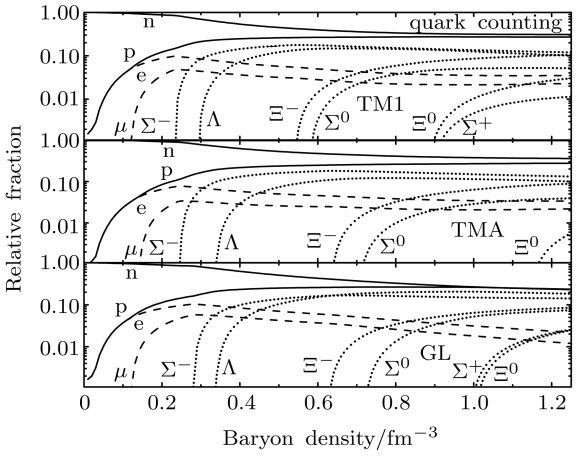


Fig.1. Relative population for quark counting choice with three nucleon parameter sets TM1, TMA, and GL.

but at a lower density ($\rho \sim 0.54\,\mathrm{fm}^{-3}$) in the case of the TM1 parameter set. The presence of the Ξ^- makes the μ_e drop even faster. The baryon and lepton populations for TM1 and GL parameter sets essentially agree with the results displayed in Ref.[15] although the hyperon coupling used was different. To summarize, only for the TM1 parameter set all the eight lightest baryons are present before $1.0\,\mathrm{fm}^{-3}$, so it seems that the parameter set TM1 favours the presence of hyperons. We obtain similar results for the other two choices for hyperon coupling.

For a certain RMF parameter set TM1, we present in Fig.2 the relative fractions predicted by adopting the three choices of hyperon coupling, namely the hyperon potential model (top panel), the quark counting (middle panel) and the universal coupling (lower panel). The threshold densities of the

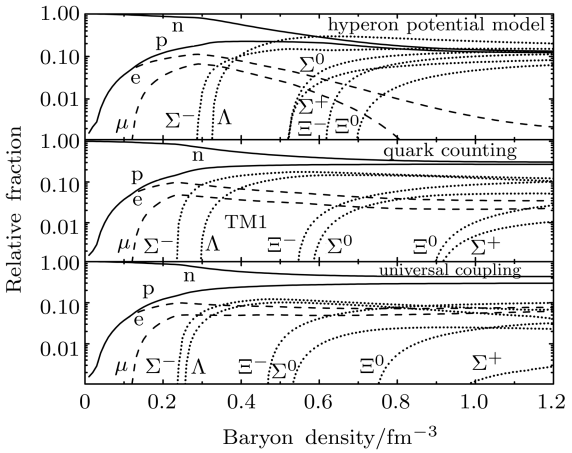


Fig.2. Relative population with nucleon parameter set TM1 for three kinds of hyperon coupling choices.

first-appearing two hyperons Σ^- and Λ are affected only slightly by different choices for hyperon couplings. In the hyperon potential model, the Λ fraction turns greater than the Σ^- fraction at $\rho \sim 0.4\,\mathrm{fm}^{-3}$, therefore it becomes the most abundant hyperon species at high densities. Whereas in the other two cases of adopting the quark counting and the universal coupling, the Λ population never grows greater than the Σ^- population. For the quark counting and the universal coupling choices, the population of nucleons is shown to dominate in the whole density region. But in the hyperon potential model, the populations of Σ^- and Λ can excess the neutron population, and the Σ^- and Λ become the dominating particles at high densities. Particularly the Λ population can attain to 1.5 times the neutron population. It is worth mentioning that under the universal coupling choice the Ξ^- hyperons become the dominant hyperons at $\rho > 0.88\,\mathrm{fm}^{-3}$, while the Λ and the Σ^- are the most abundant hyperons at high densities for the other two choices of hyperon coupling. For the GL and the TMA parameter sets, we find similar results at high densities although they are not shown in the figure. In general, the hyperons come about at lower densities and their populations are most abundant at high densities for the hyperon potential model choice. The hyperon couplings from the hyperon potential model are more favourable for the presence of hyperons than the other two adopted hyperon coupling choices.

More massive and more positive charged particles appear at higher densities, and their sequence is much more sensitive to the hyperon coupling. The most massive hyperon Ξ appears much earlier for the quark counting choice and the universal coupling choice than for the hyperon potential model because the hyperon couplings from the hyperon potential model always lead to a smaller value of μ_e especially at high densities. While in the two other cases of the quark counting and the universal coupling choices, the predicted μ_e rises monotonically as a function of density, however, with a reduced slope. Therefore, the lepton concentration is more abundant than that obtained by the hyperon potential model choice (see Fig.3). The rapid building-up of hyperons with increasing density makes the matter very strangeness-rich at high densities, with almost as many protons as neutrons.

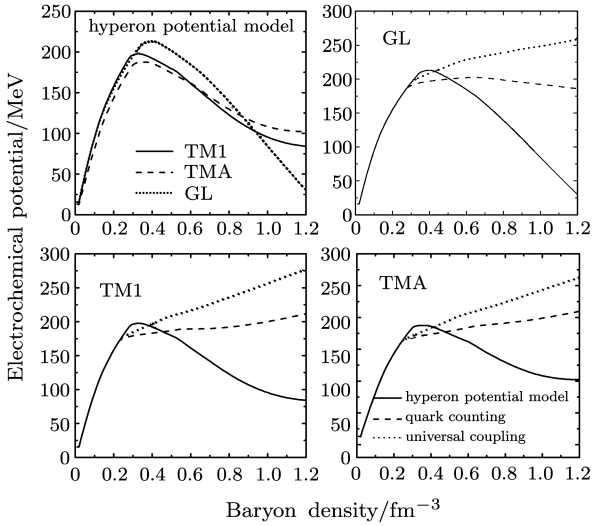


Fig.3. Electrochemical potential with three nucleon parameter sets TM1, TMA, and GL for three kinds of hyperon coupling choices.

The hyperonization of matter in the present models can also be analysed through the density dependence of the strangeness fraction. The density dependence of the fs parameter is depicted in Fig.4. For a certain choice (as an example for the quark counting choice, we find similar results for the other two choices) of hyperon couplings, at moderate densities the strangeness content is highest by adopting the TM1 parameter set, while at high densities the GL parameter set leads to the most hyperon-rich matter. The same result can also be found in Fig.1. On the other hand, for a certain parameter set TM1, the most hyperon-rich matter is obtained by adopting the hyperon potential model when the density increases up to $0.4\,\mathrm{fm}^{-3}$, which implies that the Λ hyperon plays a dominant role in hyperonization of matter in this case. From the figure we may also conclude that the hyperon potential model is the most favourable hyperon coupling choice for the presence of hyperon.

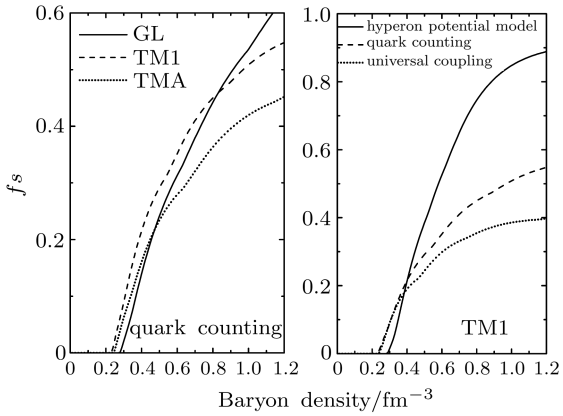


Fig.4. Strangeness fraction with three nucleon parameter sets TM1, TMA, and GL or for three kinds of hyperon coupling choices.

The effective mass of nucleon, obtained with the three nucleon parameter sets TM1, TMA, and GL for the three hyperon coupling choices, is presented in Fig.5. We see clearly its strong dependence on the adopted parameter sets. For the two parameter sets TM1 and TMA with vector self-interaction, the predicted effective masses approach to zero at high enough densities, while for the GL parameter set the effective mass of nucleon is still about 30% of the rest mass of nucleon. Similar results have been shown in Ref.[20]. In fact, the GL parameter set was proposed by Glendenning for investigating the neutron star properties. The influence of the hyperon couplings on the effective mass of nucleon is shown to be much weaker than that of the nucleon couplings. This can be readily understood since the effective mass of nucleon is related directly to the nucleon couplings, whereas the hyperon couplings affect the effective mass of nucleon only through their effects on the scalar-isoscalar potentials indirectly and thus their effects are relatively weak.

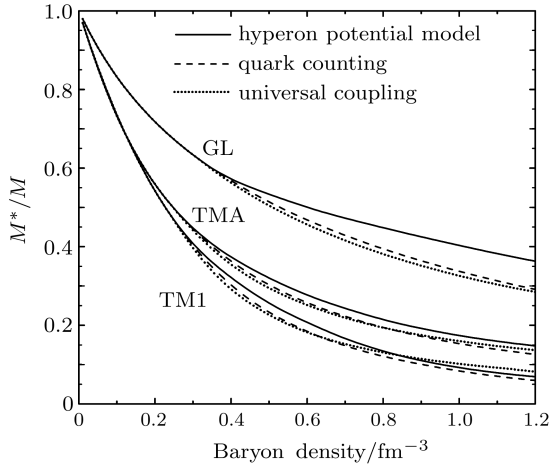


Fig.5. Effective of mass nucleon with three nucleon parameter sets TM1, TMA, and GL for three kinds of hyperon coupling choices.

We show in Fig.6 the dependences of the meson fields on the nucleon parameter sets and the hyperon couplings. Initially the ω field always rises linearly for all the three model parameter sets of TM1 TMA and GL, but slows down when hyperons are present due to the vector self-interaction for the TM1 and TMA parameterizations. The strange fields are developed rapidly with increasing density after their onset because of the presence of hyperons. For a certain parameter set TM1, the influence of hyperon couplings on the attractive σ field is less pronounced than on the repulsive ω field. The universal coupling choice leads to the strongest ω field in the whole density region, so the resulting EOS for the universal coupling choice is stiffest in spite of another vector field ϕ being weakest at high densities, therefore the nonstrange mesons still roughly dominate the global properties of the dense hyperonic matter. The result obtained by the quark counting choice is close to that by the universal coupling choice. For the hyperon potential model choice, the strength of the strange scalar σ^*-field, which provides the attraction for hyperon interaction, is strongest at high densities. But the strengths of the vector ρ-field, which gives rise to a repulsive potential in the isovector interaction channel, and vector ω-field, which brings about a short-range repulsion in nucleon interaction, both are weakest. This

choice results in very different field strengths as compared with the other two choices and consequently the EOS obtained by the hyperon potential model choice differs remarkably from those by the quark counting choice and the universal coupling choice (see Fig.7). Being different from the other two hyperon coupling choices, under the hyperon potential model choice the contribution of the strange mesons is comparable with that of nonstrange mesons at high densities. That can be easily understood since for the hyperon potential model choice, the strength of strange meson field is strong enough and the hyperons may play an important role at high densities.

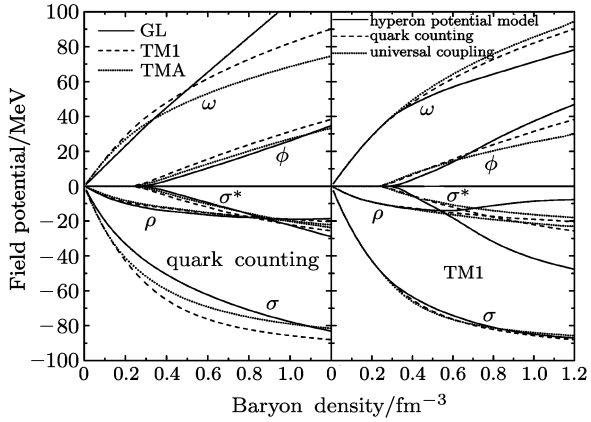


Fig.6. Field strength with three nucleon parameter sets TM1, TMA, and GL or for three kinds of hyperon coupling choices.

Figure 7 shows the effects of model parameter set and hyperon coupling on the EOS of hadronic matter at β-equilibrium. For a given hyperon coupling choice, the GL parameter set leads to the stiffest EOS in the high density region, since the vector field ω is strongest for the GL parameter set among the three adopted parameter sets. Due to a similar reason, the TMA set gives the softest EOS. For a certain parameter set TM1, the hyperon potential model provides an much softer EOS than the other two choices for the hyperon couplings since the attractive potential is strongest and the repulsive potential is weakest under the hyperon potential model choice. The investigation of the neutron star matter properties is one of the most interesting subjects in astrophysics.[28−32] For a given EOS the global properties of neutron stars can be obtained from the hydrostatic equilibrium equation of Tolman[33] and Oppenheimer and Volkoff.[34] Figure 8 shows the mass of neutron star as a function of the radius of neutron star corresponding to the EOS shown in Fig.7. In the case of quark counting choice, GL parameter set predicts the biggest maximum mass of 1.86 $M_{\rm sun}$ ($M_{\rm sun}$ stand for the mass of sun) which is about 0.2 $M_{\rm sun}$ larger than the predicted maximum mass by adopting the TMA parameter set. For the TM1 parameter set, hyperon potential model choice predicts the lowest maximum mass of 1.47 $M_{\rm sun}$ which is lower than prediction of quark counting choice 1.85 $M_{\rm sun}$ and that of universal choice 2.0 $M_{\rm sun}$. It is consistent with the result in Fig.7 that the hyperon potential model has the softest EOS among three hyperon coupling model choices.

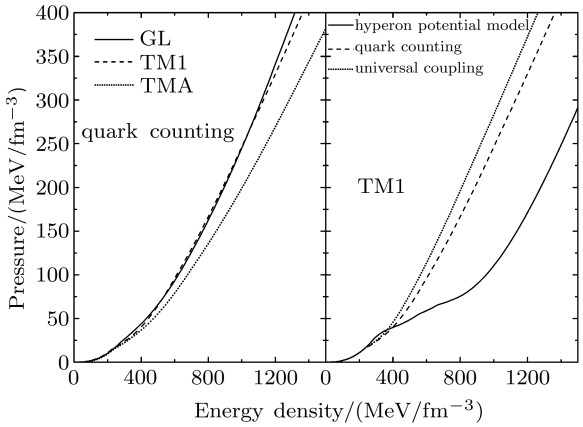


Fig.7. Equations of state with three nucleon parameter sets TM1, TMA, and GL or for three kinds of hyperon coupling choices.

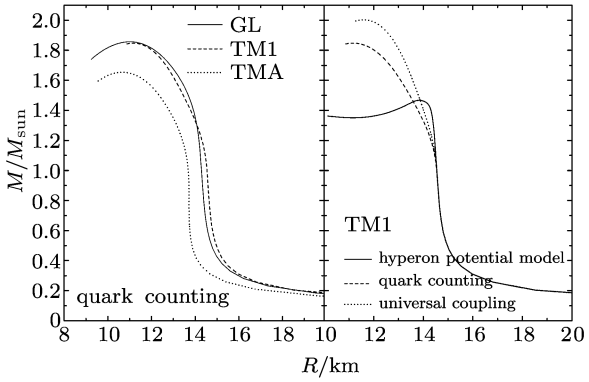


Fig.8. The mass-radius relation calculated for the three nucleon parameter sets TM1, TMA, and GL or for three kinds of hyperon coupling choices.

In summary, we have studied the effects of model parameter set and hyperon coupling choice on the properties of hadron matter at β-equilibrium. We find that the parameter set TM1 may favour the presence of hyperons most, while at high densities the parameter set GL provides the most hyperon-rich matter. As for the changing of effective mass of nucleon, the hyperon coupling influence is much weaker than that when adopting the RMF parameter set. The

nonstrange mesons still roughly dominate the global properties of the dense hyperon matter. We also find that the TMA parameter set predicts the lower maximum mass of the neutron star than other parameter sets. For a certain parameter set TM1, the most hyperon-rich matter is obtained for the hyperon potential model. It means that the hyperon potential model favours the transition from a neutron star to a hyperon star in which the hyperons are dominant.[35] The hyperon potential model also predicts the maximum mass of $1.47\,M_{\rm sun}$ which is about $0.38\,M_{\rm sun}$ lower than the prediction with quark counting choice and $0.53\,M_{\rm sun}$ lower than the prediction with universal choice.

References

[1] Glendenning N K 1982 *Phys. Lett.* B **114** 392
[2] Glendenning N K 1985 *Astrophys. J.* **293** 470
[3] Glendenning N K Z 1987 *Phys.* A **326** 57
[4] Walecka J D 1974 *Annals. Phys.* **83** 491
[5] Serot B D and Walecka J D 1986 *Adv. Nucl. Phys.* **16** 1
[6] Reinhard P G 1989 *Rep. Prog. Phys.* **52** 439
[7] Serot B D 1992 *Rep. Prog. Phys.* **55** 1855
[8] Ring P 1996 *Prog. Part. Nucl. Phys.* **37** 193
[9] Serot B D and Walecka J D 1997 *Int. J. Mod. Phys.* E **6** 515
[10] Meng J, Toki H, Zhou S G, Zhang S Q, Long W H and Geng L S 2006 *Prog. Part. Nucl. Phys.* **57** 470
[11] Schaffner J, Dover C B, Gal A, Greiner C and and Stöcker H 1993 *Phys. Rev. Lett.* **71** 1328
[12] Schaffner J, Dover C B, Gal A, Greiner C, Millner D J and Stöcker H 1994 *Ann. Phys.* **235** 35
[13] Qian W L, Su R K and Song H Q 2004 *J. Phys.* G **30** 1893
[14] Bednarek I and Manka R 2005 *J. Phys.* G **31** 1009
[15] Schaffner J and Mishustin I N 1996 *Phys. Rev.* C **53** 1416
[16] Schaffner J, Hanauske M, Stöcker H and Greiner W 2002 *Phys. Rev. Lett.* **89** 171101
[17] Glendenning N K 2000 *Compact Stars* (New York: Springer-Verlag)
[18] Moszkowski S A 1974 *Phys. Rev.* D **9** 1613
[19] Ghosh S K, Phatak S C and Sahu P K 1995 *Z. Phys.* A **352** 457
[20] Santos A M S and Menezes D P 2004 *Phys. Rev.* C **69** 045803
[21] Taurine A R, Vasconcellos C A Z, Malheiro M and Chiapparini M 2001 *Phys. Rev.* C **63** 065801
[22] Shen H 2002 *Phys. Rev.* C **65** 035802
[23] Espíndola A L and Menezes D P 2002 *Phys. Rev.* C **65** 045803
[24] Schaffner J and Gal A 2000 *Phys. Rev.* **62** 034311
[25] Sugahara Y and Toki H 1994 *Prog. Theor. Phys.* **92** 803
[26] Shen Y S and Ren Z Z 1998 *Acta Phys. Sin.* **47** 4 (in Chinese)
[27] Yadav A L, Kaushik M and Toki H 2004 *Int. J. Mod. Phys.* **13** 647
[28] Guo H, Yang S, Hu X and Liu Y X 2001 *Chin. Phys.* **10** 805
[29] Wang Q D and Lu Y 1985 *Acta Phys. Sin.* **34** 7 (in Chinese)
[30] Dai Z G and Lu Y 1994 *Acta Phys. Sin.* **43** 2 (in Chinese)
[31] Zhang J, Liu M Q and Luo Z Q 2006 *Chin. Phys.* **15** 1477
[32] Lu G C, Li Z H, Zuo W and Luo P Y 2006 *Acta Phys. Sin.* **55** 84 (in Chinese)
[33] Tolman R C 1939 *Phys. Rev.* **55** 364
[34] Oppenheimer J R and Volkoff G M 1939 *Phys. Rev.* **55** 374
[35] Jia H Y, Sun B X, Meng J and Zhao E G 2001 *Chin. Phys. Lett.* **18** 1571